Journal of Quantitative Spectroscopy & Radiative Transfer 198 (2017) 40–47

Contents lists available at ScienceDirect

Journal of Quantitative Spectroscopy & Radiative Transfer

journal homepage: www.elsevier.com/locate/jqsrt

A long term study of the relations between erythemal UV-B irradiance, total ozone column, and aerosol optical depth at central Argentina

Gustavo G. Palancar[a,*], Luis E. Olcese[a], Mariana Achad[a], María Laura López[b], Beatriz M. Toselli[a,*]

[a] Departamento de Físico Química / INFIQC / CLCM / CONICET, Facultad de Ciencias Químicas, Universidad Nacional de Córdoba, Ciudad Universitaria, 5000 Córdoba. Argentina

[b] Facultad de Matemática, Astronomía, Física y Computación / IFEG / CONICET, Universidad Nacional de Córdoba, Ciudad Universitaria, 5000 Córdoba. Argentina

ARTICLE INFO

Article history:
Received 27 December 2016
Revised 12 April 2017
Accepted 3 May 2017
Available online 4 May 2017

Keywords:
Radiation amplification factor
UV-B erythemal irradiance
Aerosols
Ozone
Radiative transfer model
Single scattering albedo

ABSTRACT

Global ultraviolet-B irradiance (UV-B, 280–315 nm) measurements made at the campus of the University of Córdoba, Argentina were analyzed to quantify the effects of ozone and aerosols on surface UV-B erythemal irradiance (UVER). The measurements have been carried out with a YES Pyranometer during the period 2000–2013. The effect of ozone and aerosols has been quantified by means of the Radiation Amplification Factor (RAF) and by an aerosol factor (AF, analogous to RAF), respectively. The overall mean RAF under cloudless conditions was (1.2 ± 0.3) %, ranging from 0.67 to 2.10% depending on solar zenith angle (SZA) and on Aerosol Optical Depth (AOD). The RAF increased with the SZA with a clear trend. Similarly, the aerosol effect under almost-constant ozone and SZA showed that, on average, a 1% increase in AOD forced a decrease of (0.15 ± 0.04) % in the UVER, with a range of 0.06 to 0.27 and no defined trend as a function of the SZA. To analyze the effect of absorbing aerosols, an effective single scattering albedo (SSA) was determined by comparing the experimental UVER with calculations carried out with the TUV radiative transfer model.

1. Introduction

The ultraviolet (UV) solar range is the most energetic solar radiation that reaches the Earth's surface, and is involved in key photochemical reactions and photo biological processes that take place in the atmosphere and the biosphere, respectively. This radiation affects human health, damages aquatic life and plants, and affects the conservation and durability of materials, in addition to impacting on the global energy balance and climate change [44]. However, not all the effects are harmful, as solar radiation is also the main factor for vitamin D synthesis, essential for bone and musculoskeletal health [18]. To quantify all the UV effects, different action spectra ($B(\lambda)$) are used, depending on the particular biological response. McKinlay and Diffey [35] established the erythemal action spectrum, which represents the spectral response of human skin to sunburn (or erythema) for wavelengths between 280 and 400 nm. The spectral incident irradiance ($I(\lambda)$) weighted with this spectrum is called erythemal radiation (UVER) [9,47], which is computed as:

$$UVER = \int B(\lambda) I(\lambda) d\lambda \quad (1)$$

Due to the above mentioned effects, ultraviolet solar radiation reaching the lower atmosphere and at the Earth's surface has extensively been studied in the last decades. UVER levels at Earth's surface are controlled by geographic (latitude, longitude, altitude, etc.) and atmospheric factors. Among the latter, the most important are clouds, ozone and atmospheric aerosols. Other pollutants, such as SO_2 and NO_2, can also affect the UVER levels but in a lesser extent.

As in the case of UV-B irradiance (280–315 nm), the daily course of the UVER at the surface (the bell shape) is driven by the variation of the Solar Zenith Angle (SZA). During the day, the short term variability is mainly controlled by changes in the cloud cover [2,8]. For clear sky days, the Total Ozone Column (TOC) is the main attenuating factor, being its influence highly wavelength dependent, since the ozone absorption shows a steep increase at wavelengths shorter than 330 nm [5]. The impact of ozone depletion on UVER values is frequently expressed by means of the Ra-

* Corresponding authors.
E-mail addresses: palancar@fcq.unc.edu.ar (G.G. Palancar), tosellib@fcq.unc.edu.ar (B.M. Toselli).

http://dx.doi.org/10.1016/j.jqsrt.2017.05.002
0022-4073/

diation Amplification Factor (RAF), defined as the percentage of increase in UVER that would result from a 1% decrease in the TOC [34]. In this sense, RAF was proposed and it has become a widely used standard index during the last two decades. McKenzie et al. [34] found that an ozone reduction of 1% leads to a 1.25% increase in UVER. Koepke et al. [24] showed that UVER dependence on TOC varies with the SZA. In fact, Kim et al. [22] found RAF values in the range 1.32–1.62 for SZA between 30° and 60° at Seoul, Korea.

The remaining important factor attenuating the UVER that reaches the surface is the aerosol loading. While the relation between ozone and surface UVER appears to be well established, less is known about the effects of aerosols. The effect of aerosols on UVER is complex owing to the variety of composition of material that may be present in the atmosphere, as well as its varying size distribution and optical properties [46]. The largest reductions in UV irradiance are associated with dust and smoke plumes from Africa and South America [42]. The magnitude of the aerosol effect can be large (UV irradiance at the surface can be reduced by more than 50% [45]) and highly variable, depending on the number of particles and their physical and chemical properties [12].

An alternative approach to quantify the levels of UVER on the surface of the planet is the UV Index (UVI). This simple and widely used parameter is an important resource to raise awareness and warn the population about the risks of overexposure to the Sun [48]. This index has an open-ended scale and it is calculated multiplying the UVER by 40 m^2 W^{-1}. The WHO together with the World Meteorological Organization (WMO), have established a universal scale for UVI with five intervals: <2 (low erythemal risk), 3–5 (moderate), 6–7 (high), 8–10 (very high) and >11 (extreme). It is important to stand out that during intervals with extreme values, an exposition to solar radiation of 2–4 min is enough to generate redness and even burning of the skin (for individuals with skin type I).

Systematic investigations on the temporal variation of UV-B radiation and the influencing parameters in South America are still sparse [10,27]. In Córdoba, Argentina, Palancar and Toselli [38–40] investigated the daily and seasonal behavior of UV-B and UVER for the period November 1998- December 2002. However, and due to the combined effect of all these parameters in controlling the UV-B levels, the precise determination of the role of the controlling parameters is quite difficult.

In this study we investigated the impact of ozone and atmospheric aerosols on surface UVER at different SZA at Cordoba City, Argentina. Data analyzed included surface UVER measured by UV pyranometers from January 2000 to December 2013 and the Aerosol Optical Depth (AOD) retrieved by a nearby AERONET site (Cordoba-CETT). The Tropospheric Ultraviolet Visible (TUV) radiative transfer model [28] was used to retrieve the single scattering albedo (SSA) from the AERONET AOD and the UV-B measurements. The aim of this study is to evaluate the effects of the variability of ozone and aerosols on the surface erythemal ultraviolet irradiance, covering a wide range of SZAs and for an extended period of time.

2. Instrumentation, data modeling and methodology

2.1. Solar irradiance measurements

Irradiance measurements were carried out by using a pyranometer YES (Yankee Environmental System, Inc.) model UVB-1, which measures UV-B global irradiance (280–315 nm). The UVB-1 spectral response function is given elsewhere [38]. The uncertainties in the irradiance measurements are mainly related to the instrument geometry and materials used to build it. Uncertainties are intrinsic to the instrument measurement system (temperature control, transmittance and sensitivity of the different filters, cosine response, spectral response, etc.), which lead to a maximum of 5% difference between two identical calibrated instruments as described in the work of Dichter et al. [14]. At low Sun (large SZA), the reflection in the horizontal receiving surface of the instrument becomes more important, leading to additional uncertainties. Thus, SZA larger than 75° were not considered in this study. More details about uncertainties, calibration, and maintenance of the pyranometer can be found in López et al. [26]. Observations were recorded as half a minute averages values. Cloudless conditions were periodically assured by direct observers (3 to 5 times a day). Because visible and infrared wavelengths are more sensitive to cloud presence, the daily course of total irradiance (300–3000 nm), measured with a YES model TSP-700 pyranometer, was qualitatively used to double check the cloudless condition at all times. The instruments were mounted on a wide-open area in the University Campus in Córdoba City, Argentina (31.4° S, 64.18° W), located southwest of downtown, and were placed on a cement yard surrounded by low buildings, trees, grass, paved streets and bare soil.

2.2. Data

In order to evaluate the sensibility of UVER on ozone and aerosols, TOC and AOD (340 nm) data were required. TOC values were obtained daily by the Total Ozone Mapping Spectrometer (TOMS) instrument onboard Earth Probe spacecraft until 2005 and by the Ozone Monitoring Instrument (OMI) onboard Aura spacecraft since 2006. The data were provided by the Ozone Processing Team of the Goddard Space Flight Center of the National Aeronautic and Space Administration (NASA, United States). AOD values were taken from a nearby AERONET station (about 28 km away from the UVER measurement site). The AOD was measured with a CIMEL Electronique 318A Sun photometer at the Cordoba-CETT station (31.52° S, 64.46° W). Since 1999, this AERONET station provided measurements of AOD at seven spectral bands (340, 380, 440, 500, 670, 870 and 1020 nm). The station was operating until December 2010, when the photometer was deployed at another region away from Córdoba. A complete statistical characterization of the aerosol optical parameters for all the operational years of this station can be found in the comprehensive work of Olcese et al. [37]. A detailed description of the instruments, data acquisition procedure, and calibration is given in Holben et al. [20,21]. An accuracy assessment of the AERONET retrievals can be found in the work of Dubovik et al. [15]. Andrada et al. [3] confirmed that the aerosols present in this AERONET site have the same origin and characteristics as those present in the site where the UVER measurements were carried out, i.e. they have a regional character and allowed to directly consider the characteristic of local aerosols in model calculations. All AOD values used in this work were level 2.0 version 2 and at 340 nm. Uncertainty in the AOD values at this wavelength was estimated to be 0.02 [16].

2.3. UVER modeling

The TUV model version 4.1 was used for all UVER calculations [28]. A sensitivity analysis was carried out using this model in order to establish the best values for the most important parameters for Córdoba City [39]. The final setup used in the model was as follows: the wavelength grid was built with 1 nm intervals between 280 and 315 nm; the surface albedo was assumed to be Lambertian, wavelength independent, and with a constant value of 0.05 throughout the year (there are no snowfalls in Córdoba City); the extraterrestrial irradiance values were taken from Van Hoosier et al. [43] and Neckel and Labs [36]. An 8-stream discrete ordinate method and cloudless sky conditions were used. To run the model we used as input parameters the AOD from AERONET and the TOC from TOMS/OMI (as described in Section 2.2).

2.4. Methodology

Changes in the UVER due to TOC variations were analyzed at different SZA using RAF. The RAFs are unitless coefficients used to estimate the effects of the reduction in the ozone column on the incident UVER. The effect of the O_3 changes depends on the spectral overlap between the action spectrum and the irradiance. It is called an amplification factor because if the ozone changes, even larger changes in UVER can occur. For small changes in the TOC (a few percent) the effects can be described by a simple proportionality, i.e. the percent rule (e.g. [7,29]):

$$RAF = -\frac{\Delta UVER/UVER}{\Delta TOC/TOC} \quad (2)$$

However, as the effect of ozone on UVER is not linear, the percent rule fails for larger changes in TOC. In these cases it is better to integrate the power law [30,33] which leads to:

$$UVER \sim \mathrm{TOC}^{-\mathrm{RAF}} \quad (3)$$

or

$$\mathrm{RAF} = -\frac{\Delta \ln(UVER)}{\Delta \ln(TOC)}, \quad (4)$$

where Δln(TOC) is the difference between the natural logarithms of two TOCs and Δln(UVER) is the difference of the natural logarithms of the corresponding irradiances. Thus, in this work, RAFs have been calculated with this more generally applicable power law formulation. Mathematically, the RAF is simply the slope of the regression line on a log-log plot. A physical interpretation of the RAF (for action spectra decaying exponentially) would be the ratio of the action spectrum decay rate to the O_3 absorption cross section decay rate [33].

To quantify the effects of aerosols on UVER we plotted UVER vs. AOD for different 14-DU-wide intervals of TOC (252 ± 7, 267 ± 7, 282 ± 7, 297 ± 7, and 312 ± 7 DU) and at SZA between 10° and 70° in intervals of 2° (plots not shown). For each SZA we fit these data to three different functions: linear, power (i.e. analogous to RAF), and exponential decay. Here, it should be kept in mind that because of the variation along the year of the TOC, the SZA (with a minimum of 55° during winter time), and the AOD, not all the combinations had enough data points to fit a curve. For most of the available combinations the r^2 coefficient values for the three functions were similar. For example, the average (for all the TOC ranges) r^2 coefficients at SZA $(51 \pm 1)°$ were 0.77, 0.78, and 0.79 for linear, power and exponential functions, respectively. These results are probably related to the large dispersion shown in the plots and also to the small variability in the AOD at Córdoba, where the maximum values at 340 nm are around 0.7 but the average is just 0.17 ± 0.07 [37]. With these restrictions in mind, and as the differences in the r^2 coefficients were negligible, we decided to use the power function, which has the form:

$$UVER = A\ (AOD)^B \quad (5)$$

or

$$ln(UVER) = B\ ln(AOD) + \ln A \quad (6)$$

where A and B are fitting parameters. As Eq. (5) is analogous to the power law, this allows us to compare the relative effects of ozone or aerosols on UVER in a similar way. Thus, the fitting parameter B, from now on named Aerosol Factor (AF), is analogous to RAF, i.e. it is the slope of the plot of ln(UVER) vs. ln(AOD). However, it should be noted that expression 5 is just a fit of the relation between broadband erythemal measurements and its corresponding AOD at given SZAs and TOCs. We are not just replacing TOC by AOD in the RAF definition, as RAF was derived using different considerations. This can be seen in the work of Micheletti et al. [33], where a simple analytic expression for RAF is derived (see the Appendix in that work). Among the used approximations, aerosols are considered inside a tropospheric factor, T_{trop} (together with Rayleigh scattering and clouds), which is assumed to be independent of wavelength in the UV range. This is supported by the fact that, compared to ozone, aerosol optical depth in the UV-B range has a much weaker dependence with wavelength.

3. Results and discussion

This section is organized as follows: in Section 3.1 we present the daily and annual cycle of UVER for all the years of the campaign together with a discussion of the Ultraviolet Index (UVI) values reached along the measurement period. Section 3.2 presents the dependence of UVER on TOC and Section 3.3 presents the dependence of UVER on AOD.

3.1. UVER levels

3.1.1. Daily cycle

UVER was analyzed for the period January 2000 to December 2013. In Córdoba City, the daily variation of UVER is mainly controlled by the SZA, cloudiness and aerosol loading, as the ozone concentration usually exhibits small day-to-day variations [40].

Fig. 1 shows the daily variation of experimental and modeled UVER for three selected days under different conditions: (a) clear sky (cloudless sky and no aerosol loading) (31 Oct 2001); (b) cloudless sky with a moderate aerosol loading (27 Oct 2009); (c) cloudless sky with a high aerosol loading (19 Sep 2001). In the three cases model calculations are for clear sky conditions.

As can be seen in Fig. 1(a) for a clear sky day, the evolution of UVER along the day is given only by the SZA. In addition, it is important to note the very good agreement between experimental and calculated values, which were found to be better than ±5% for SZA <50° and ±10% for SZA between 50° and 70° for clear sky days [40]. For that reason, when a noticeable difference between experimental and modeled values is observed, this difference can be attributed to the specific meteorological conditions of the particular day. That is the case of aerosol loaded days, as is shown in Fig. 1(b) and (c) where a clear reduction of the experimental UVER, in relation to a modeled clear sky day, is observed. For 19 Sep 2001, the attenuation has a mean value of 20% and reaches up to 37% at low Sun (average AOD = 0.7). The small variations observed in model calculations (e.g. panels a and b) are known numerical instabilities coming out from the 8-stream calculation [41]. However, they affect neither the analysis nor the results of the present work.

3.1.2. Annual cycle

The annual and inter-annual variability of UVER is determined by the different meteorological situations, along with the annual variation of TOC. Fig. 2(a) shows the experimental and calculated UVER values at solar noon (between 13:00 and 13:31 h, local time) for the complete considered period. We chose the solar noon (i.e. the time of the day with the maximum UVER) because of the potentially harmful effects of high UVER levels. The absence of data during 2004–2005 was due to problems in the measurement site which prevent to conduct the UVER measurements. The observed dispersion of the data can be attributed to the specific atmospheric conditions of each day and at that time showing the effects of meteorology on the agreement against the clear sky model. For the considered period, UVER experimental values vary from a minimum of 0.03 W m^{-2} to a maximum of 0.38 W m^{-2} with a mean value of 0.19 W m^{-2}. Fig. 2(b) shows the ratio between experimental and the clear sky calculated values. Values <1 are attributed to the presence of aerosols or clouds that attenuate the experimental UVER, while values >1 are due to cloud enhancement events

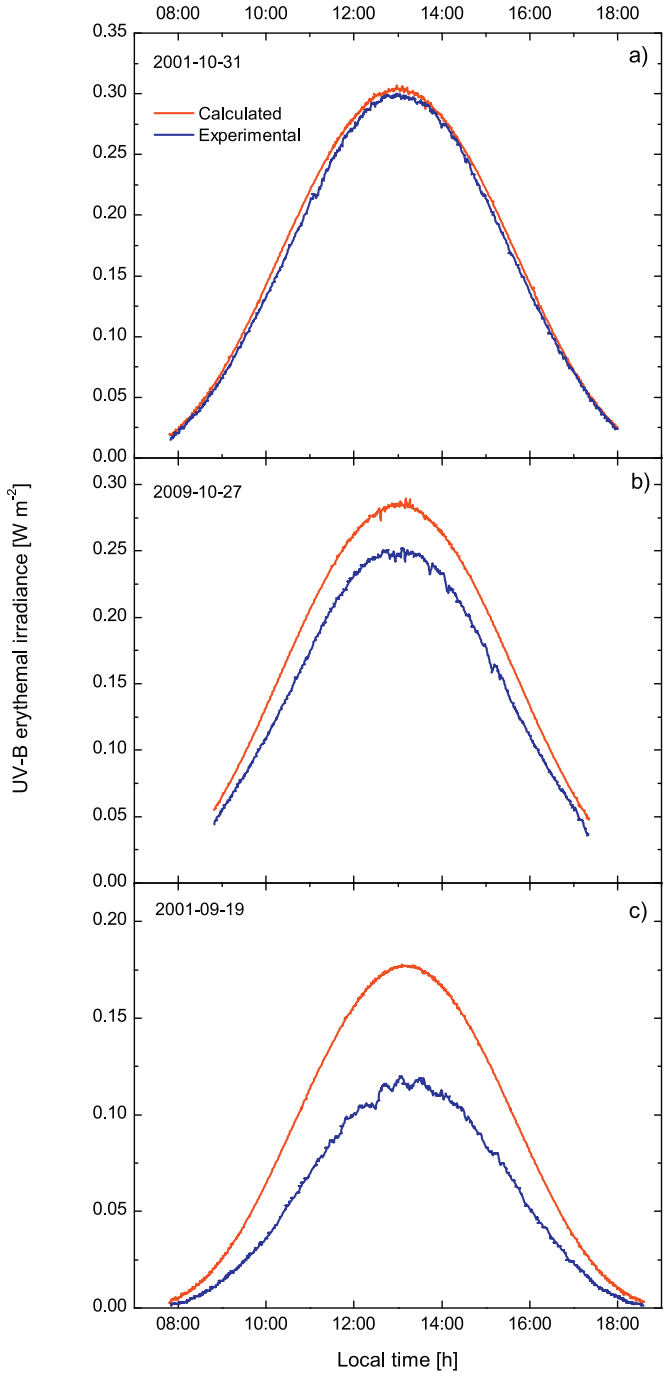

Fig. 1. Daily course of experimental and calculated (TUV) UVER (280–315 nm) at Córdoba for cloudless days and a) no aerosols, b) moderate aerosol load and c) high aerosol load. Model calculations are for clear sky conditions.

(broken clouds) or due to the expected agreement between measurements and calculations. This agreement was shown to be better than 5% for SZA less than 50° and better than 10% for ZSA less than 70° for clear sky days [40].

Fig. 3 shows the monthly means of UVER at the solar noon for the whole period. As seen, the maximum value is observed in January, even though the minimum in the SZA variation is in December. This is due to the TOC variation, which shows a maximum around September and then decreases to its minimum around April, shifting the maximum in radiation from December to January. The annual and interannual variation of TOC (as monthly averages) at Córdoba during the campaign period (2000–2013) is

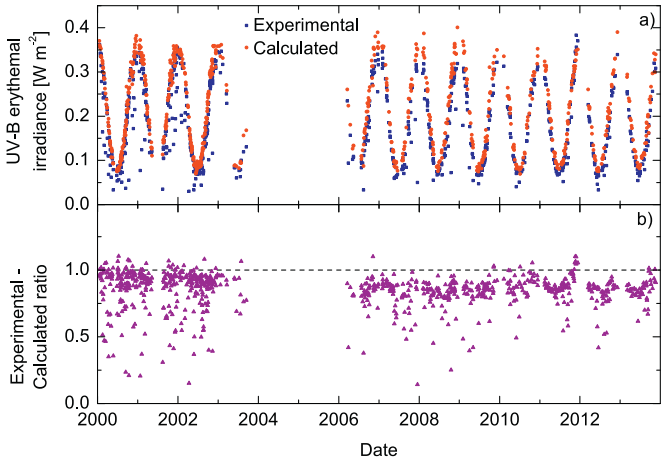

Fig. 2. (a) UVER (280–315 nm) at solar noon during the 2000–2013 campaign. Measurements (YES UVB-1) and clear sky model calculations (TUV). (b) Measurement/model ratio.

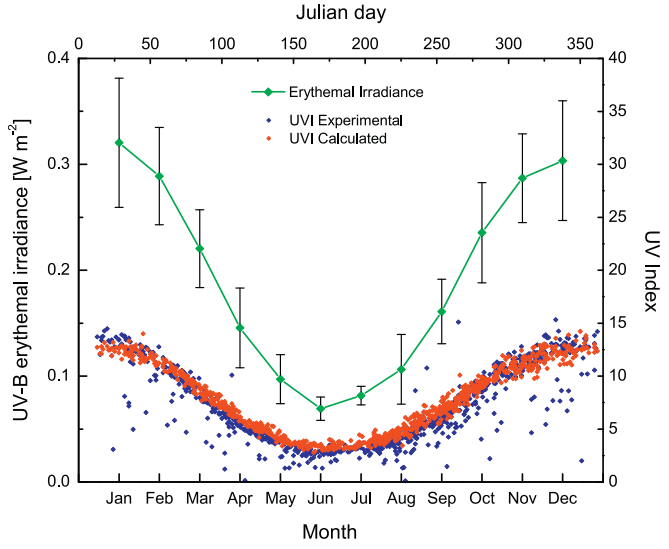

Fig. 3. Annual variation of UVER (280–315 nm, as monthly averages of all years) and UVI (at solar noon) at Córdoba. Errors bars correspond to one standard deviation.

shown in Fig. 4. As seen in Fig. 3, the minimum UVER value is observed in June. In average, typical winter values are only about 9–17% of the summer values. The differences between summer and winter for each year (derived from the maximum and minimum UVER measurements, respectively) are shown in Table 1. The values suggest small changes between consecutive years. However, as the period is not long enough (less than 15 years) and a gap is present, it is not possible to define a trend.

As mentioned before, a related variable to quantify the levels of UVER at the surface is the UV Index, which can be calculated from the UVER experimental values. However, UVI under clear sky conditions can also be calculated by using the formula

$$UVI \sim 12.5\ \mu_o^{2.42}\left(\frac{TOC}{300}\right)^{-1.23} \quad (7)$$

where μ_o is the cosine of the SZA. In this formula, proposed by Madronich [31], the TOC (in DU) is divided by 300, which was arbitrarily chosen as the reference condition. Instead, we used 282 DU, as it is the average of the TOC values for the days used in this work (see Fig. 4). The annual variation of the experimental and calculated (through Eq. (7)) UVI at the solar noon is shown in Fig. 3.

Table 1
Summer-Winter differences in UVER (280–315 nm) for all the years in the campaign.

Year	2000	2001	2002	2006	2007	2008	2009	2010	2011	2012	2013
Difference ($W\,m^{-2}$)	0.329	0.320	0.316	0.307	0.295	0.264	0.275	0.273	0.331	0.306	0.266

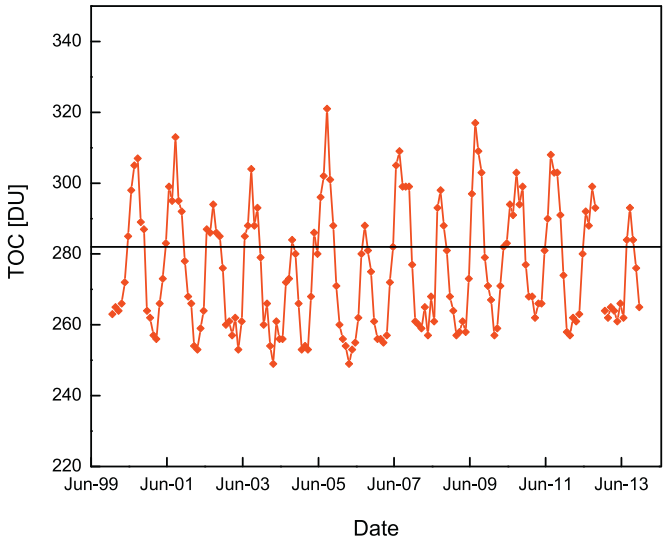

Fig. 4. Annual and inter annual variation (as monthly averages) of the total ozone column at Córdoba during the measurement campaign. The horizontal line shows the average of TOC values for the days used in this work (282 DU).

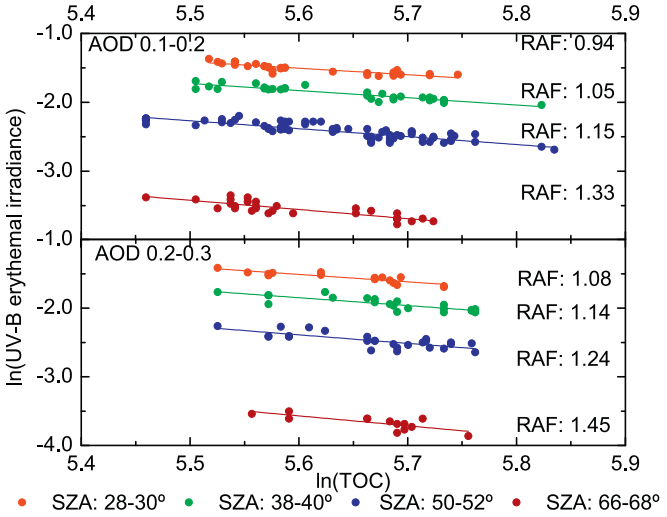

Fig. 5. Effect of TOC variation on UVER (280–315 nm) for different AOD and SZA ranges. UVER values are for cloudless days. RAF values, calculated from the slopes, are also shown. All slopes have r^2 values larger than 0.5.

Here, it is important to highlight that the formula was developed for cloudless and unpolluted conditions and our experimental measurements reflect all the sky conditions. This is probably the reason of the small underestimations and overestimations observed for high and low UVI values, respectively. Even though, and despite the simplicity of Eq. (7), results observed in this figure show, at a glance, a general reasonable agreement along the whole year and for all the SZA and TOC used in this work (SZA between 8° and 55° and TOCs between 232 DU and 355 DU). As in the UVER case, the relatively large standard deviation is mostly due to the effect of clouds. As UVI is calculated from UVER, both plots in Fig. 3 follow the same pattern. From November to March, UVI in Córdoba was found to be in the extreme range (greater than 11). It is in its minimum (around 3) during winter time (June–August) and reaches the level high (7–9) during spring and fall time (October-November and April-May, respectively).

3.2. Dependence of UVER on TOC

RAF coefficient is defined considering that all the factors affecting the UVER, except TOC, remain constant. This situation can be easily considered in model calculations but it is far away from reality as aerosols are almost always present, limiting seriously the number of clear sky experimental data. Madronich [29] points out that some atmospheric factors, such as cloud cover, surface albedo, elevation, and aerosols, among others, have small effects on RAFs, as they change all wavelengths in a similar proportion. Thus, in our work, the RAFs were calculated (from measurements) for AOD varying from 0 to 0.6 in 0.1 intervals and SZAs from 10° to 70° in 2° intervals. The range of total ozone values included in the RAF calculation was from 260 to 325 DU, because these are the values usually present in the region (see Fig. 4). As an example, Fig. 5 shows the relationship between ln(UVER) and ln(TOC) (i.e. Eq. (4)) for cloudless days, at several SZAs and in two AOD ranges (0.1–0.2 and 0.2–0.3). As it was mentioned before, although AOD in Córdoba can reach values up to 0.7, there are not enough episodes to perform a valid analysis with the highest values. The slopes of the lines were calculated to estimate the RAFs. The goodness of a fit is given by the coefficient of determination (r^2) which had to be higher than 0.5 to be accepted.

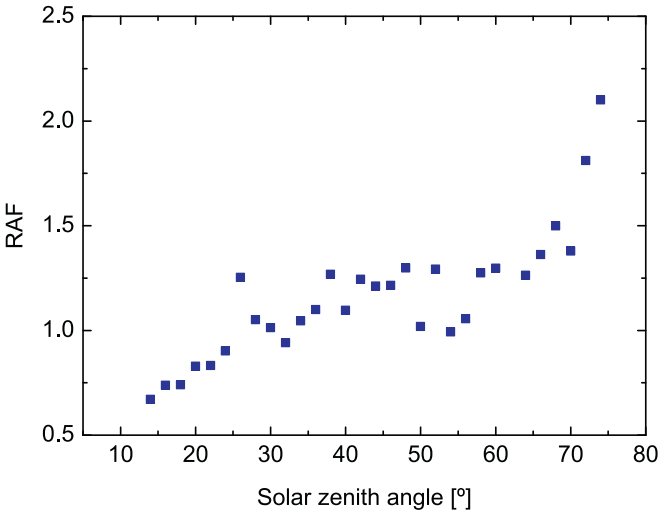

Fig. 6. Dependence of RAF with the SZA at all AOD.

All the calculated RAFs are shown as a function of SZA in Fig. 6. When more than one RAF value was available for each SZA, the average was calculated. The average RAFs for cloudless skies lie in the range from 0.67 to 2.10 depending on AOD and SZA. Results found in the literature about the behavior of RAF as a function of SZA are ambiguous. While model calculations show a decrease with the increasing SZA (which is the expected result, e.g. [33]) several other works have shown the opposite trend when using experimental measurements. Unfortunately, in none of these works the reasons of these findings are analyzed or explained [6,13,19,34].

As recognized in [29], even the power rule has serious limitations, as it is an oversimplified representation of several and complex atmospheric processes, some of them wavelength dependent. In our case, the results show a clear increase of RAF with the increasing SZA. Although we did not find a conclusive explanation, either, these results could be related to relatively systematic changes in atmospheric factors along the day (e.g. aerosol loading and properties or ozone distribution aloft) and or uncertainties in experimental measurements (TOC, broadband UV-B irradiance or approximate conversion factors provided by the manufacturer). Here, we discarded the uncertainties caused when the longest wavelengths of the action spectrum are neglected (usually in the UV-A range) as we are using only the UV-B range. The overall mean RAF showed that 1% decrease of total ozone forces an increase of (1.2 ± 0.3) % in the UVER. This mean RAF is comparable with the values reported by the other works [4,13,17,22,25]. The variations depending on SZA and on AOD could be attributed to scattering/absorbing effects of aerosols.

3.3. Dependence of UVER on AOD

To analyze the effects of aerosols on UVER we used Eq. (6), which is analogous to Eq. (4). As mentioned in Section 2.4, plots of UVER vs AOD presented a large dispersion, which was associated to variations in the SSA of the aerosols. Therefore, to understand how these optical property influences AF, the slopes have been evaluated according to the SSA in two intervals (0.8–0.89 and 0.9–0.99) and at different SZA and TOC. In a previous work we found that the site is affected by a mixture of at least two types of aerosols (urban and mineral) which are present along the year in different combinations [1]. Therefore, to fit the results to a straight line, the effect for that particular combination (AOD and SSA) needed to be considered. Thus, for every SZA interval the results are separated according to the SSA value.

As the SSA at 340 nm is not provided by AERONET, we estimated the aerosol SSA using a simple method (e.g. [11,32]). First, another set of UVER model calculations was performed incorporating the aerosol optical properties taken from AERONET in the TUV model (AOD and asymmetry parameter (g) set to 0.66). Andrada et al. [3] showed that this g value is appropriate to describe the local aerosols in the UV-B range. Each calculation is repeated for different SSA varying from 0.6 to 0.99 (with 0.01 resolution). This range was chosen following the SSA values determined by AERONET at 440 nm for Córdoba region [37]. Then, every calculation was compared with the corresponding experimental value. The selected SSA value was that which makes the difference closer to zero, provided this difference is less than 5%. This threshold value was chosen as a function of the model-measurement agreement shown in Palancar and Toselli [40].

Fig. 7 shows the effect of aerosols on the surface UVER for a fixed SZA interval, $(51 \pm 1)^{o}$, different TOCs, and discriminated in two ranges of SSA (0.8–0.89 and 0.9–0.99). In this way, the effects of absorption and scattering by aerosols are also considered. Similar plots were performed for SZA varying between 10° and 70° (not shown). The slopes of the plots (i.e. the AF) ranged from 0.06 to 0.27 under the given experimental conditions. The correlations are well described by a linear relationship as in the total ozone case, with an average slope and standard deviation of 0.15 ± 0.04 for cloudless days. All the r^2 of the curves presented in this figure show statistically significant correlation between ln(UVER) and ln(AOD) at almost constant SZAs and TOC. As expected, the result shows that the effect of aerosols is generally larger when SSA is smaller; that is, absorbing aerosols have larger effect on the reduction of surface erythemal UV-B radiation than scattering aerosols.

Another important observation is that there is no clear trend as a function of the SZA as shown in Fig. 8. At first sight this result seems surprising because dependence with the cosine of SZA is expected. However, this result is in agreement with other published works. Kim et al. [23] determined that the parameter named cloudless sky AOD RAF varies in the range of 0.18 to 0.37 depending on total ozone and SZA with a mean value of 0.23. In that work, the AOD RAF values were almost independent of the SZA.

In our work, the impact of aerosols on UVER was 10–15% of the ozone effect. Although AOD effect is smaller than ozone effect (quantified by RAF parameter), aerosol properties (e.g. SSA) should be taken into consideration for better understanding the surface UVER changes and their effects on the atmosphere and the biosphere.

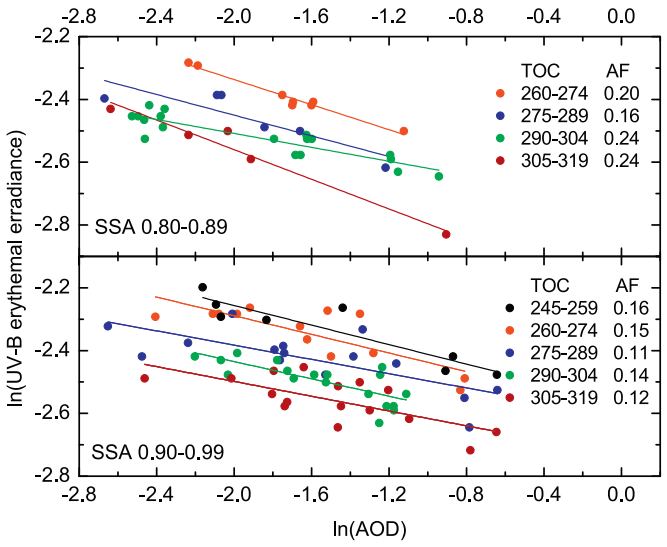

Fig. 7. Effect of aerosols (AOD) on UVER (280–315 nm) for different TOC, at two SSA ranges and SZA=$(51 \pm 1)°$. UVER values are for cloudless days. The Aerosol Factor values (AF), calculated from the slopes, are also shown. All slopes have r^2 values larger than 0.5.

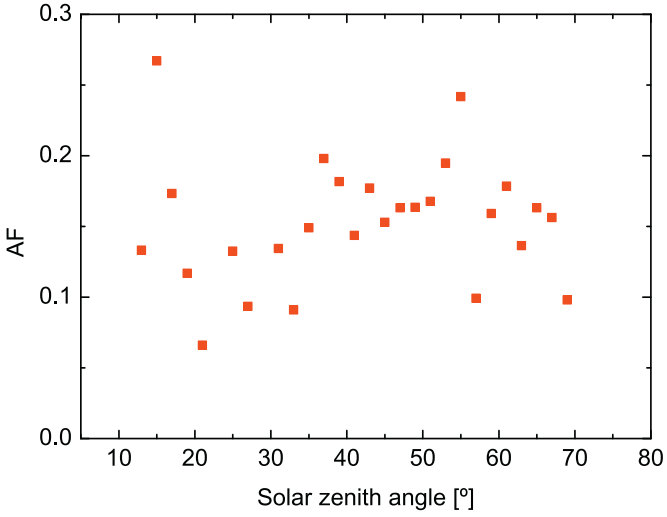

Fig. 8. Dependence of Aerosol Factor (AF) with the SZA for all the SSA values (0.6–0.99) and all the TOC values.

4. Concluding remarks

In this work, we used the UV-B erythemal irradiance (280–315 nm) measured at Córdoba City, Argentina during 2000–2013 to analyze and quantify the effects of the variability in the total ozone column and aerosols as a function of SZA.

The effect of ozone on UVER was assessed based on RAF calculations. The RAF under cloudless conditions suggests that a 1% decrease in the total ozone forces, in average, an increase of (1.2 ± 0.3)% in the UVER irradiance with a range of 0.67 to 2.10% depending on SZAs (10–70°) and on AODs (<0.6). The RAFs for cloudless sky cases show increasing values with the SZA. This pattern is opposite to what it is expected from model calculations but similar to results of other previous experimental studies. This situation highlights the need of more studies to determine the reasons of this disagreement. The effect of aerosols on UVER was first analyzed by fitting the plots of UVER vs. AOD to different functions. As the power function was selected, plots of ln(UVER) vs. ln(AOD) were build for different TOCs, SSAs and SZAs using the slopes of these plots (named Aerosol Factor, AF) to quantify the aerosol effect. Similarly to the analysis for RAFs, the results showed that under cloudless conditions a 1% increase of AOD forces a decrease of only (0.15 ± 0.04) % in the UVER, with the values ranging from 0.06 to 0.27%, depending on SZA, TOC and SSA. It was also found that absorbing aerosols (SSA between 0.8 and 0.89) have larger effects than scattering aerosols (SSA between 0.9 and 0.99). The AF appears to be almost independent on SZAs. The effect of aerosols is small compared to the effect of ozone but AOD can vary largely in a short period of time. The sensitivities of UVER irradiance due to the AOD variations are, in the mean, weaker by 6.6 times to those due to total ozone changes.

Although the observed O_3 and aerosol effects show a good agreement with other works, the calculated values should be considered valid only for Córdoba as it is widely recognized that different conditions (particularly TOC and SZA) can lead to different coefficients.

Acknowledgments

We thank CONICET (PIP 2013-2015 grant number 1120120100004CO), Secretaría de Ciencia y Tecnología-Universidad Nacional de Córdoba (grant number 05/C275) and ANPCYT (PICT 2014- 0876) for partial support of the work reported here. We thank the AERONET principal investigator Brent Holben for establishing and maintaining the site used in this investigation. Mariana Achad thanks CONICET for a postdoctoral fellowship.

References

[1] Achad M, López ML, Palancar GG, Toselli BM. Retrieving the relative contribution of aerosol types from single particle analysis and radiation measurements and calculations: a comparison of two independent approaches. J Aerosol Sci 2013;64:11–23.
[2] Alados-Arboledas L, Alados I, Foyo-Moreno I, Olmo FJ, Alcántara A. The influence of clouds on surface UV erythemal irradiance. Atmos Res 2003;66:273–90.
[3] Andrada GC, Palancar GG, Toselli BM. Using the optical properties of aerosols from the AERONET database to calculate surface solar UV-B irradiance in Córdoba, Argentina: comparison with measurements. Atmos Environ 2008;42:6011–19.
[4] Bilbao J, Román R, Yousif C, Mateos D, de Miguel A. Total ozone column, water vapour and aerosol effects on erythemal and global solar irradiance in Marsaxlokk, Malta. Atmos Environ 2014:508–18.
[5] Bais A, Zerefos C, Meleti C, Ziomas I, Tourpali K. Spectral measurements of solar UVB radiation and its relations to total ozone, SO2, and clouds. J Geophys Res 1993;98:5199–204.
[6] Blumthaler M, Salzgeber M, Ambach W. Ozone and ultraviolet-B irradiances: experimental determination of the radiation amplification factor. Photochem Photobiol 1995;61(2):159–62.
[7] Booth CR, Madronich S. Radiation amplification factors: Improved formulation accounts for large increases in ultraviolet radiation associated with Antarctic ozone depletion. Ultraviolet radiation in Antarctica: measurements and biological effects. Weiler CS, Penhale PA, editors. Washington, D. C.: American Geophysical Union; 1994.
[8] Calbó J, Pagés D, González J. Empirical studies of cloud effects on UV radiation: a review. Rev Geophys 2005;43:RG2002.
[9] C.I.E.. Commission internationale de l'Eclairage, erythema reference action spectrum and standard erythema dose, Vienna, Austria: CIE Central Bureau; 1998. CIE S007E-1998.
[10] Cordero RR, Seckmeyer G, Damiani A, Jorquera J, Carrasco J, Muñoz R, et al. Aerosol effects on the UV irradiance in Santiago de Chile. Atmos Res 2014;149:282–91.
[11] Corr CA, Krotkov N, Madronich S, Slusser JR, Holben B, Gao W, et al. Retrieval of aerosol single scattering albedo at ultraviolet wavelengths at the T1 site during MILAGRO. Atmos Chem Phys 2009;9:5813–27.
[12] De Bock V, De Backer H, Van Malderen R, Mangold A, Delcloo A. Relations between erythemal UV dose, global solar radiation, total ozone column and aerosol optical depth at Uccle, Belgium. Atmos Chem Phys 2014;14:12251–70.
[13] de Miguel A, Román R, Bilbao J, Mateos D. Evolution of erythemal and total shortwave solar radiation in Valladolid, Spain: effects of atmospheric factors. J Atmos Solar-Terrestrial Phys 2011;73:578–86.
[14] Dichter BK, Beaubien AF, Beaubien DJ. Development and characterization of a new solar ultraviolet irradiance detector. J Atmos Oceanic Technol 1993;10:337–44.
[15] Dubovik O, Smirnov A, Holben BN, King MD, Kaufman YJ, Eck TF, et al. Accuracy assessments of aerosol optical properties retrieved from AERONET sun and sky-radiance measurements. J Geophys Res 2000;105:9791–806.
[16] Eck TF, Holben BN, Reid JS, Dubovik O, Smirnov A, O'Neill NT, et al. Wavelength dependence of the optical depth of biomass burning, urban, and desert dust aerosols. J Geophys Res 1999;104(D24):31333–49.
[17] Esteve AR, Martínez-Lozano JA, Marín MJ, Estellés V, Tena F, Utrillas MP. The influence of ozone and aerosols on the experimental values of UV erythemal radiation at ground level in Valencia. Int J Climatol 2009;29:2171–82.
[18] Fioletov VE, McArthur LJB, Mathews TW, Marrett L. On the relationship between erythemal and vitamin D action spectrum weighted ultraviolet radiation. J Photochem Photobiol 2009;95:9–16.
[19] Guarnieri RA, Padilha LF, Guarnieri FL, Echer E, Makita K, Pinheiro DK, et al. A study of the anticorrelations between ozone and UV-B radiation using linear and exponential fits in southern Brazil. Adv Space Res 2004;34:764–8.
[20] Holben BN, Eck TF, Slutsker I, Tanre D, Buis JP, Setzer A, et al. AERONET-a federated instrument network and data archive for aerosol characterization. Remote Sens Environ 1998;66:1–16.
[21] Holben BN, Tanré D, Smirnov A, Eck TF, Slutsker I, Abuhassan N, et al. An emerging ground-based aerosol climatology: aerosol optical depth from AERONET. J Geophys Res 2001;106:12067–97.
[22] Kim JE, Ryu SY, Kim YJ. Determination of radiation amplification factor of atmospheric aerosol from the surface UV irradiance measurement at Gwangju, Korea. Theor Appl Climatol 2008;91:217–28.
[23] Kim JE, Cho H-K, Mok J, Yoo HD, Cho N. Effects of ozone and aerosol on surface UV radiation variability. J Photochem Photobiol B 2013;119:46–51.
[24] Koepke P, Reuder J, Schwander H. Solar UV radiation and its variability due to the atmospheric components. Recent Res Develop Photochem Photobiol 2002;6:11–34.
[25] Lee YG, Koo J-H, Kim J. Influence of cloud fraction and snow cover to the variation of surface UV radiation at King Sejong station, Antarctica. Atmos Res 2015;164–165:99–109.
[26] López ML, Palancar GG, Toselli BM. Effects of stratocumulus, cumulus, and cirrus clouds on the UV-B diffuse to global ratio: experimental and modeling results. J Quantit Spectrosc Radiat Transfer 2012;113:461–9.
[27] Lovengreen L, Fuenzalida H, Villanueva L. Ultraviolet solar radiation at Valdivia, Chile (39.83S). Atmos Environ 2000;34:4051–61.
[28] Madronich S. Photodissociation in the atmosphere: 1. Actinic flux and the effects of ground reflections and clouds. J Geophys Res 1987;92:9740–52.
[29] Madronich S. The atmosphere and UV-B radiation at ground level. In: Environmental UV photobiology. New York: Plenum; 1993. p. 1–39.
[30] Madronich S, McKenzie RL, Bjorn LO, Caldwell MM. Changes in biologically active ultraviolet radiation reaching the Earth's surface. J Photochem Photobiol B 1998;46:5–19.
[31] Madronich S. Analytic formula for the clear-sky UV Index. Photochem Photobiol 2007;83:1537–8.
[32] Medina R, Fitzgerald RM, Minc Q. Retrieval of the single scattering albedo in the El Paso-Juarez Airshed using the TUV model and a UV-MFRSR radiometer. Atmos Environ 2012;46:430–40.
[33] Micheletti MI, Piacentini RD, Madronich S. Sensitivity of biologically active UV radiation to stratospheric ozone changes: Effects of action spectrum shape and wavelength range. Photochem Photobiol 2003;78(5):456–61.
[34] McKenzie R, Matthews W, Johnston P. The relationship between erythemal UV and Ozone derived from spectral irradiance measurements. Geophys Res Lett 1991;18:2269–72.
[35] McKinlay AF, Diffey BL. A reference action spectrum for ultraviolet induced erythema in human skin. Commission Internationale de l'Eclairage (CIE) 1987;6:17–22.
[36] Neckel H, Labs D. The solar radiation between 3300 and 12500Å. Solar Phys 1984;90:205–58.
[37] Olcese LE, Palancar GG, Beatriz MToselli. Aerosol optical properties in Central Argentina. J Aerosol Sci 2014;68:25–37.
[38] Palancar GG, Toselli BM. Erythemal ultraviolet irradiance in Córdoba, Argentina. Atmos Environ 2002;36:287–92.
[39] Palancar GG, Toselli BM. Effects of meteorology and tropospheric aerosols on UV-B radiation: a 4-year study. Atmos Environ 2004;38:2749–57.
[40] Palancar GG, Toselli BM. Effects of meteorology on the annual and interannual cycle of the UV-B and total radiation in Cordoba City, Argentina. Atmos Environ 2004;38:1073–82.

[41] Palancar GG, Fernandez RP, Toselli BM. Photolysis rate coefficients calculations from broadband UV-B irradiance: model-measurement interaction. Atmos Environ 2005;39:857–66.
[42] Tarasick DW, Fioletov VE, Wardle DI, Kerr JB, McArthur LJB, McLinden CA. Climatology and trends of surface UV radiation: Survey article. Atmos Ocean 2003;41(2):121–38.
[43] Van Hoosier ME, Bartoe JD, Brueckner GE, Printz DK. Solar irradiance measurements 120-400 nm from space lab-2. Vancouver: IUGG Assembly; 1987.
[44] UNEP (United Nations Environment Programme), 2010. Environmental effects of ozone depletion and its interactions with climate change: 2010 assessment. ISBN 92-807-2312-X.
[45] Walter C, Freitas SR, Kottmeier C, Kraut I, Rieger D, Vogel H, et al. The importance of plume rise on the concentrations and atmospheric impacts of biomass burning aerosol. Atmos Chem Phys 2016;16:9201–19.
[46] Wan X, Kang S, Xin J, Liu B, Wen T, Wang P, et al. Chemical composition of size-segregated aerosols in Lhasa city, Tibetan Plateau. Atmos Res 2016;174–175:142–50.
[47] Webb AR, Slaper H, Koepke P, Schmalwieser AW. Know your standard: clarifying the CIE erythema action spectrum. Photochem Photobiol 2011;87:483–6.
[48] WHO. Global solar UV Index. Geneva, Switzerland: World Health Organization; 2002. p. 1–28. Publication WHO/S-DE/OEH/02.2.